No: 17572-H
Please mark the appropriate section for this paper
☐ Experimental
☐ Clinical

ANTICANCER RESEARCH *46*: xxx-xxx (2026)
doi: 10.21873/anticanres.xxxxx

Immunohistochemical Expression and Clinicopathological Assessment of PD-1, PD-L1, NY-ESO-1, and MAGE-A4 Expression in Desmoid Tumor

KAZUHIKO HASHIMOTO[1], SHUNJI NISHIMURA[1], HIROKI TAN[1], TOMOHIKO ITO[2] and KOJI GOTO[1]

[1]Department of Orthopedic Surgery, Kindai University Hospital, Sakai, Japan;
[2]Department of Orthopedic Surgery, Kindai Nara University Hospital, Ikoma, Japan

Abstract

Background/Aim: The action of immune molecular mechanisms in the intratumor microenvironment in desmoid tumors (DTs) remains unclear. The purpose of this research was to clarify the expression patterns of PD-1/PD-L1 immune checkpoint pathways and NY-ESO-1/MAGE-A4 molecular pathways in DTs.

Materials and Methods: Immunohistochemical analysis of CD4, CD8, PD-1, PD-L1, NY-ESO-1, and MAGE-A4 were carried out on biopsy specimens collected from patients with DT managed at our hospital. In addition, relationships between the expression frequencies of each immune marker were explored.

Results: In this study, four male and five female patients were recruited, with a mean age of 37.0 years (range=11-84 years). The average ± S.D. percentage of cells positive for β-catenin, CD4, CD8, PD-1, PD-L1, NY-ESO-1, and MAGE-A4 was 43.9±18.9, 14.6±6.80, 0.75±4.70, 0±0, 5.1±6.73, 30±21.6, and 68.9±20.8, respectively. β-catenin correlated moderately and positively with CD4 (r=0.49), weakly and positively with PD-L1 (r=0.25), and strongly and positively with NY-ESO-1 (r=0.52). CD4 showed a moderate positive correlation with PD-L1 (r=0.36), while NY-ESO-1 correlated moderately and positively with MAGE-A4 (r=0.42).

Conclusion: The NY-ESO-1/MAGEA4 immune pathway may play a more prominent role than the PD-1/PD-L1 checkpoint pathway within the tumor microenvironment of DT.

Keywords: PD-1, PD-L1, NY-ESO-1, MAGE-A4, desmoid tumor.

Introduction

Desmoid tumors (DTs), also referred to as invasive fibromas, are monoclonal neoplasms derived from myofibroblasts that originate in the muscle, tendon, or neural stroma (1). Morphologically, these tumors consist of small, bland, elongated spindle-shaped cells lacking distinct cytoplasmic borders (2). In the most recent WHO classification of soft tissue and bone tumors, DTs are categorized as intermediate-grade neoplasms, characterized by locally aggressive growth into adjacent normal tissues and only rarely by metastasis (3, 4). The invasive behavior of DTs is demonstrated by their tendency to infiltrate and encase surrounding structures, which

Kazuhiko Hashimoto, Department of Orthopedic Surgery, Kindai University Hospital, 1-14-1 Mihara-dai, Minami-ku, Sakai, Osaka 590-0197, Japan. Tel: +81 722887222, e-mail: hazzhiko@med.kindai.ac.jp

Received November 30, 2025 | Revised December 30, 2025 | Accepted December 31, 2025

can pose a serious threat when they develop near major blood vessels or vital organs (5, 6). The pathogenesis of desmoid tumors (DTs) remains incompletely understood. Previous studies have demonstrated that approximately 85% of DTs harbor somatic mutations in the β-catenin gene, *CTNNB1* (7). In addition, DTs have been reported to arise in association with inherited disorders such as familial adenomatous polyposis (FAP) syndrome (8, 9). Both *CTNNB1* and *APC* are components of the Wnt signaling pathway, and mutations in these genes lead to upregulation of β-catenin, which accumulates within the nucleus and activates transcription factors downstream in the Wnt pathway (10). Therapeutic strategies for DTs are diverse. Depending on the site of the lesion and the patient's overall condition, reported treatment modalities include surgery, chemotherapy, and radiation therapy (11). In many instances, desmoid tumors recur with greater aggressiveness following therapeutic intervention. Consequently, for patients with stable and asymptomatic disease, the most appropriate management strategy is careful observation, commonly referred to as the "watchful waiting" or "wait-and-see" approach (12). The management of DTs therefore remains challenging, and their locally invasive potential underscores the need for novel therapeutic modalities. The programmed death-1/programmed death ligand-1 (PD-1/PD-L1) immune checkpoint axis has recently been implicated in the pathogenesis of a variety of malignancies (13, 14). Moreover, anti-PD-1/PD-L1 agents have been approved for clinical use in several cancers, including melanoma and renal cell carcinoma (15, 16). Furthermore, recent findings have highlighted that the majority of 84 cancer/testis antigen proteins (CTAs), which are uniquely co-expressed in testicular germ cells and malignant cells, contribute to cancer cell proliferation and survival, thereby attracting considerable attention (17). CTAs represent a class of tumor-associated antigens whose physiological expression is confined to male germ cells of the testis and absent in adult somatic tissues (18). Beyond their tissue-restricted expression, CTAs share several defining characteristics: organization as multigene families, frequent localization to the X chromosome, transcriptional activation through hypomethylation and histone acetylation, immunogenicity in patients with cancer, heterogeneous protein expression across tumor types, and a probable association with tumor progression (14). Importantly, CTA-derived epitopes are recognized by autologous T lymphocytes directed against cancer cells. Consequently, over the past decade, CTAs have emerged as promising therapeutic targets in malignant disease (19). Among them, New York esophageal squamous cell carcinoma-1 (NY-ESO-1) is a highly immunogenic CTA linked to both innate and vaccine-induced immune responses, which may translate into clinically meaningful antitumor effects (20). Aberrant expression of NY-ESO-1 has been documented in a variety of malignancies, including hepatocellular carcinoma, esophageal carcinoma, melanoma, and non-small cell lung cancer (21). The melanoma antigen gene (MAGE) protein family constitutes a large and highly conserved group of proteins characterized by a shared MAGE homology domain (22). MAGE-A represents a CTA and belongs to the Type I MAGE subgroup, which in humans encompasses the MAGE-A, MAGE-B, and MAGE-C subfamilies, all of which are clustered on the X chromosome (23). Although the expression of most MAGE proteins is physiologically restricted to reproductive tissues, similar to NY-ESO-1, they have been reported to be aberrantly expressed in numerous cancers. Among these, MAGE-A4 is broadly expressed across diverse tumor types, with reported frequencies of 60% in esophageal cancer, 47% in ovarian cancer, 19-35% in lung cancer, 22% in colorectal cancer, and 13% in breast cancer (23, 24). Recently, we reported the involvement of PD-1/PD-L1 in aggressive soft tissue sarcomas (25). However, the literature addressing the role of PD-1/PD-L1 immune checkpoint mechanisms in DTs remains limited and controversial (5, 26). Accordingly, the objective of the present study was to characterize and elucidate the significance of PD-1/PD-L1 immune checkpoint expression, as well as the CTAs NY-ESO-1 and MAGE-A4, in DTs.

Materials and Methods

Study specimens, processing, and antigen retrieval. Immunohistochemical staining for CD4, CD8, PD-1, PD-L1, NY-ESO-1, and MAGE-A4 was conducted on pathological specimens obtained at biopsy from patients with DTs (n=9) treated at our institution between April 2006 and December 2012. The staining procedure followed previously described protocols (25). Tissue samples were fixed in formalin and embedded in paraffin. Sections of 4 μm thickness were prepared and mounted on slides. After deparaffinization and rehydration, endogenous peroxidase activity was blocked using 3% hydrogen peroxide. For antigen retrieval, PD-1 was subjected to heat treatment (95°C, 5 min) under low pH (6.0), whereas the other antigens were heat-treated (95°C, 5 min) under high pH (9.0).

Immunostaining procedure and microscopic evaluation. The sections were incubated with the following primary antibodies: CD4 (rabbit monoclonal, SP35; Roche Diagnostics, Risch-Rotkreuz, Switzerland) for 32 min at 37°C following 60 min high-pH (9.0) activation; CD8 (rabbit monoclonal, C8/144B; Nichirei Corporation, Tokyo, Japan) for 32 min at 37°C after 60 min high-pH activation; PD-1 (mouse monoclonal, ab52587; NAT105/Abcam, Cambridge, UK) for 30 min at 37°C following 30 min low-pH (6.0) activation; PD-L1 (rabbit monoclonal, ab205921; 28-8/Abcam) for 32 min at 37°C after 60 min high-pH activation; NY-ESO-1 (mouse monoclonal, E978; Santa Cruz Biotechnology, Santa Cruz, CA, USA) for 32 min at 37°C; and MAGE-A4 (rabbit monoclonal, ab229011; Abcam) for 16 min at 37°C. Sections were subsequently incubated with the appropriate secondary antibodies for 30 min at 37°C. Signal detection was performed using 3,3-diaminobenzidine (DAB) (DAB Substrate Chromogen System; DAKO, Kyoto, Japan), followed by hematoxylin counterstaining. Tonsil tissues served as positive controls; negative controls were omitted, as lymphocyte-associated antigens are broadly expressed in human tissues. Slides were examined microscopically (BIOREVO BZ-9000; KEYENCE, Osaka, Japan), with positive staining identified by the presence of brown granules in the cytoplasm, nuclei, or cell membrane.

Quantification. Quantification of immune marker expression was performed in four representative high-power fields (40× magnification) (25). The positivity rate for each marker was defined as the ratio of positively stained cells to the total number of cells. Quantification was carried out using the analysis software provided with the BIOREVO BZ-9000 system (KEYENCE). Additionally, correlations among the positivity rates of the individual immune molecules were assessed.

Statistical analysis. The positivity rates of each marker were plotted, and correlation diagrams were generated. The coefficient of determination (R) was obtained by fitting regression lines to assess the degree of correlation among the molecules. Correlation testing was performed using the Pearson's method. Associations between clinical parameters and positivity rates of each marker were analyzed in the same manner. Correlation strength was classified as follows: very strong ($1.0 \geq |R| \geq 0.7$), strong ($0.7 \geq |R| \geq 0.5$), moderate ($0.5 \geq |R| \geq 0.4$), medium ($0.4 \geq |R| \geq 0.3$), weak ($0.3 \geq |R| \geq 0.2$), and none ($0.2 \geq |R| \geq 0.0$). Survival analysis was conducted using the Kaplan–Meier method to estimate 3-year survival rates. All statistical analyses were performed with Stat Mate version 5.05 (ATMS, Tokyo, Japan).

Results

Patient characteristics. The clinical profiles of the patients included in this study are presented in Table I. A total of four male and five female individuals were recruited. The mean age was 37.0 years (range=11-84 years). The average maximum tumor diameter measured 6.08 cm (range=1.0-22.3 cm). Tumor localization was in the extremities in three cases and in the trunk in six cases.

Immunohistochemical expression. β-catenin staining was observed predominantly in the cytoplasm of tumor

Table I. *Demographic and clinical features of the study cohort.*

Factor	Patients, n
Age (years)	
Median	37
Range	11-84
Sex	
Male	4
Female	5
Tumor site	
Arms	3
Trunk	6
Tumor size (cm)	
<5	5
5-10	3
>10	1
Treatment	
Wide resection	7
Marginal resection	2

cells (Figure 1A). CD4 (Figure 1B) and CD8 (Figure 1C) immunoreactivity was mainly detected in lymphocytes infiltrating the tumor tissue. PD-1 expression was absent in all specimens (data not shown). PD-L1 staining was primarily localized to DT tumor cells (Figure 1D). NY-ESO-1 and MAGE-A4 exhibited staining within the nucleus, cytoplasm, and infiltrating lymphocytes of DT tumors (Figure 1E and F). The mean ± S.D. positivity rates for β-catenin, CD4, CD8, PD-1, PD-L1, NY-ESO-1, and MAGE-A4 were 43.9±18.9, 14.6±6.80, 0.75±4.70, 0±0, 5.1±6.73, 30±21.6, and 68.9±20.8, respectively (Table II).

Correlation between immune molecules. A moderate positive correlation was observed between β-catenin and CD4 (r=0.49, Figure 2A). No significant correlation was detected between β-catenin and CD8 (r=0.06, data not shown). β-catenin demonstrated a weak positive correlation with PD-L1 (r=0.25, Figure 2B) and a strong positive correlation with NY-ESO-1 (r=0.52, Figure 2C). In contrast, β-catenin showed a negative correlation with MAGE-A4 (r=0.13, data not shown). CD4 and CD8 were negatively correlated (r=0.13, data not shown). CD4 exhibited a medium positive correlation with PD-L1 (r=0.36, Figure 2D). CD8 was negatively correlated with PD-L1 (r=–0.13, data not shown). PD-L1 demonstrated negative correlations with NY-ESO-1 (r=–0.10, data not shown) and MAGE-A4 (r=–0.11, data not shown). NY-ESO-1 and MAGE-A4 showed a moderate positive correlation (r=0.42, Figure 2E). MAGE-A4 also exhibited a medium positive correlation with CD4 (r=0.34, Figure 3A). Finally, NY-ESO-1 demonstrated a strong positive correlation with CD8 (r=0.58, Figure 3B).

Discussion

Because the immune molecular mechanisms underlying DTs remain unclear, the present study investigated the PD-1/PD-L1 immune checkpoint axis and the expression of NY-ESO-1 and MAGE-A4 in DTs. Mutations in *β-catenin* gene are considered the principal driving force in DT pathogenesis (26). DTs generally exhibit limited intratumoral lymphocyte infiltration, with low or absent PD-1 and PD-L1 expression, and demonstrate *β-catenin* activation that appears unaffected by checkpoint inhibition (26, 27). Conversely, two-thirds of patients with DT have been reported to show PD-L1 positivity, although no significant survival differences were observed between PD-L1–positive and –negative cases (27). In the current study, tumor-infiltrating lymphocytes were identified, and PD-L1 expression was detected in 7 of 9 cases, suggesting that PD-L1–mediated immune mechanisms may contribute to DT biology. A prior report indicated NY-ESO-1 positivity in only 14.3% of DT cases (28). In contrast, all patients in the present cohort demonstrated positivity for both NY-ESO-1 and MAGE-A4. The mean cellular positivity rates were approximately 30% for NY-ESO-1 and 69% for MAGE-A4. Compared with earlier studies, the positivity rates for NY-ESO-1 and MAGE-A4 were higher, which may in part reflect the reliance on immunohistochemical staining in this investigation.

NY-ESO-1 and MAGE-A4 were implicated in both the tumor microenvironment and the pathogenesis of DTs. In our previous work, we demonstrated that PD-1/PD-L1 immune checkpoint pathways and NY-ESO-1/MAGE-A4 immune mechanisms are interconnected in soft tissue sarcomas (29, 30). In the present study, no correlation was

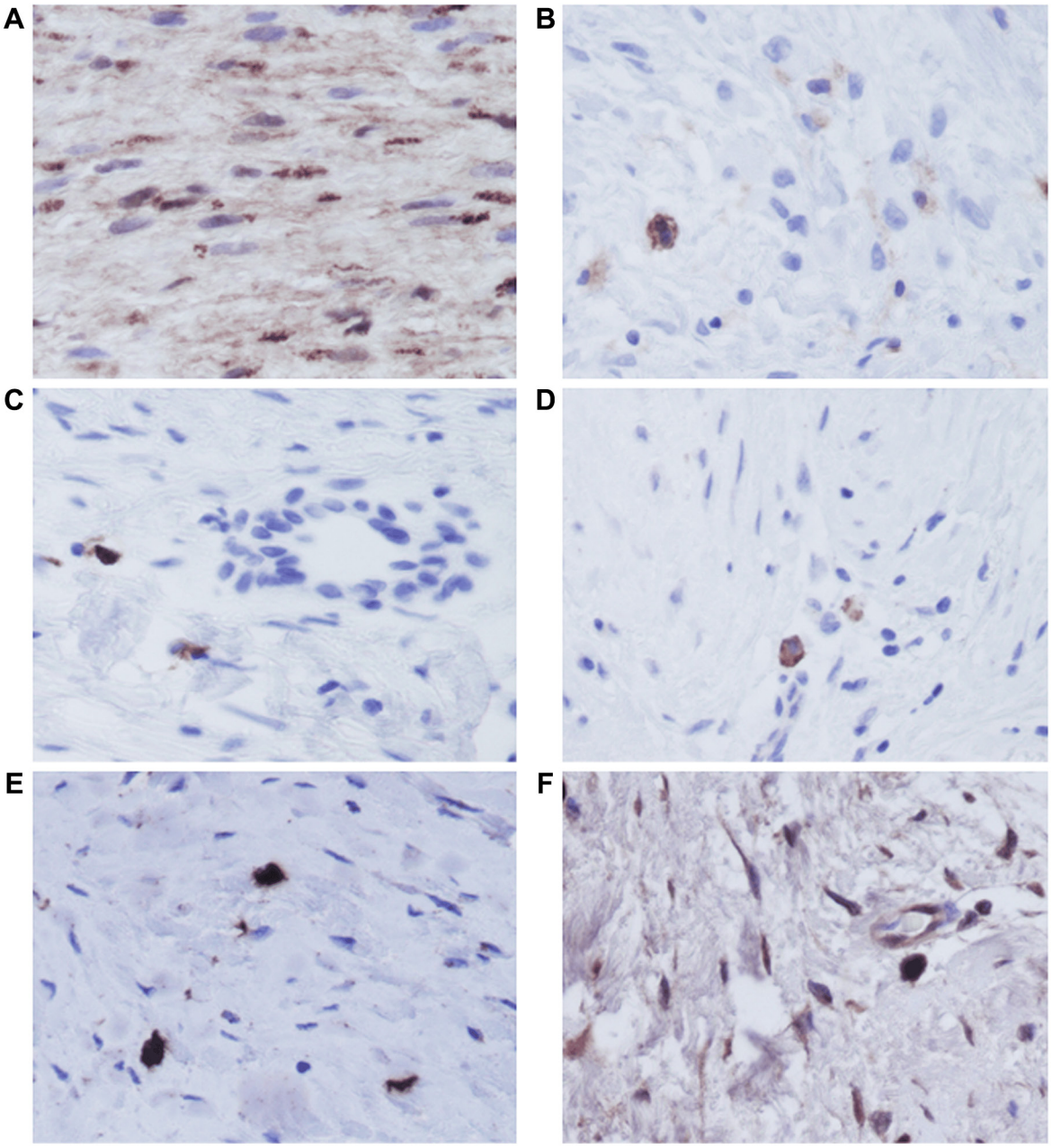

Figure 1. *Representative immunohistochemical images demonstrating positive staining for β-catenin (A), CD4 (B), CD8 (C), PD-L1 (D), NY-ESO-1 (E), and MAGE-A4 (F) are shown. β-catenin immunoreactivity is predominantly localized to the cytoplasm of tumor cells (A). CD4 (B) and CD8 (C) positivity is observed in lymphocytes infiltrating the tumor tissue. PD-L1 expression is mainly detected in DT tumor cells (D). Both NY-ESO-1 and MAGE-A4 exhibit staining within the nucleus, cytoplasm, and infiltrating lymphocytes of DT tumors (E and F).*

identified between PD-L1 expression and either NY-ESO-1 or MAGE-A4 positivity. By contrast, a significant correlation was observed between the positivity rates of NY-ESO-1 and MAGE-A4. These findings suggest that, within the DT tumor microenvironment, the PD-1/PD-L1 checkpoint axis and the NY-ESO-1/MAGE-A4 immune mechanism may function

Table II. *Rates of positive cells for immune molecules.*

Immune molecule	β-catenin	CD4	CD8	PD-1	PD-L1	NY-ESO-1	MAGE-A4
Positive cell rate (mean±S.D.)	43.9±18.9	14.6±6.80	0.75±4.70	0±0	5.1±6.73	30±21.6	68.9±20.8

PD-1: Programmed cell death 1; PD-L1: programmed death-ligand 1; NY-ESO-1: New York esophageal squamous cell carcinoma 1; MAGE-A4: melanoma-associated antigen A4; S.D.: standard deviation.

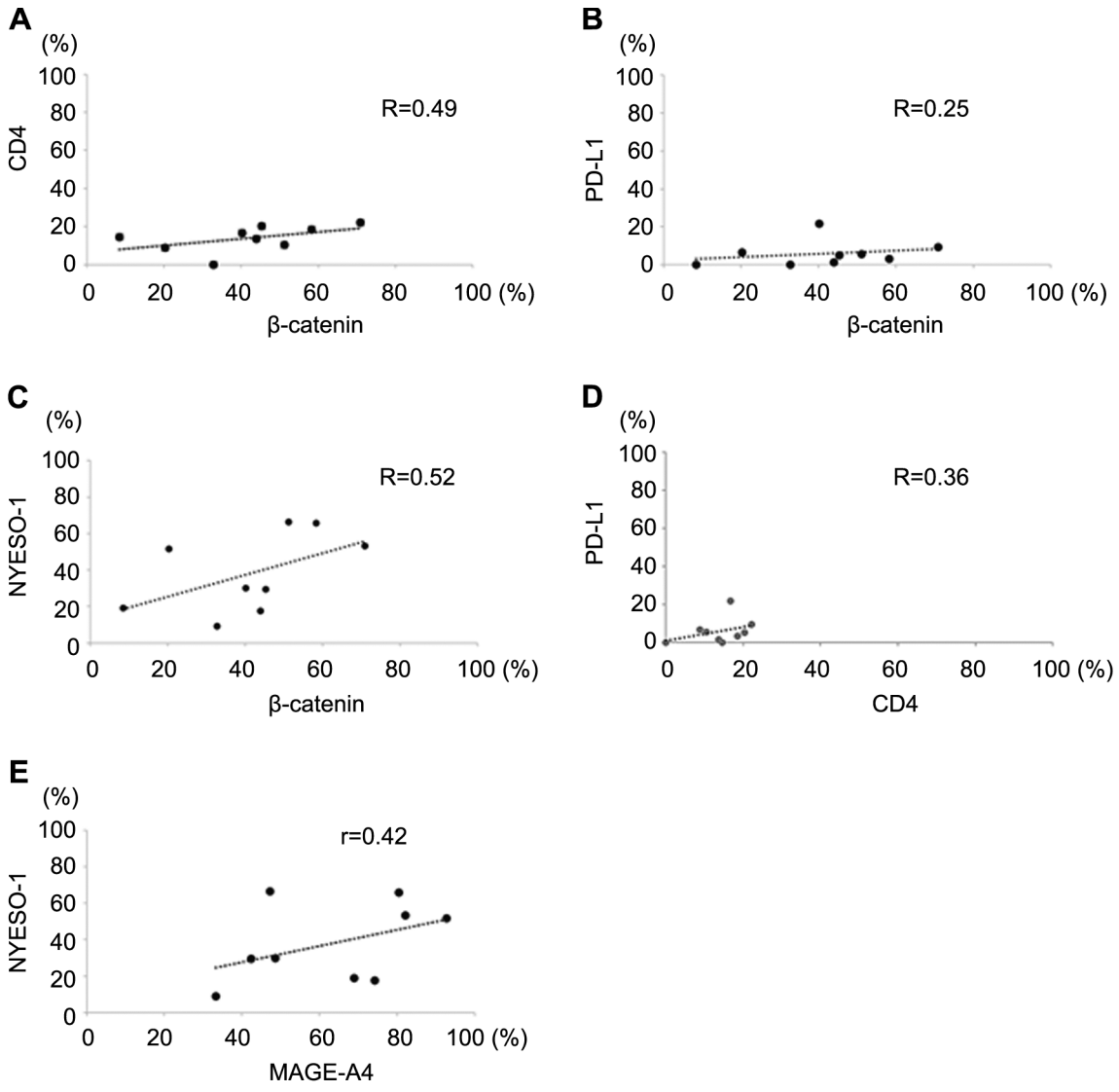

Figure 2. *Correlation plots of positive cell rates for various immune molecules are shown (A-E). A moderate positive correlation is observed between β-catenin and CD4 (r=0.49, A). β-catenin exhibits a weak positive correlation with PD-L1 (r=0.25, B) and a strong positive correlation with NY-ESO-1 (r=0.52, C). CD4 demonstrates a medium positive correlation with PD-L1 (r=0.36, D). NY-ESO-1 and MAGE-A4 display a moderate positive correlation (r=0.42, E).*

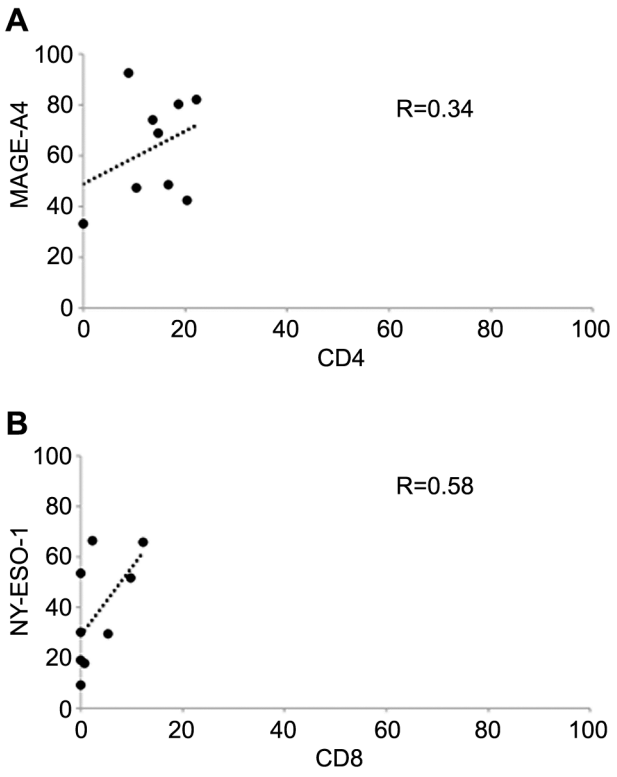

Figure 3. *Correlation plots of positive cell rates for selected immune molecules are presented (A and B). A medium positive correlation is observed between MAGE-A4 and CD4 (r=0.34, A). A strong positive correlation is observed between NY-ESO-1 and CD8 (r=0.58, B).*

independently. The observed correlation between NY-ESO-1 and MAGE-A4 further indicates that these antigens may exert a stronger influence than the PD-1/PD-L1 immune checkpoint mechanism.

Study limitations. First, the relatively small sample size may have influenced the statistical power and the robustness of the findings. Second, as the analysis relied solely on immunohistochemistry, the gene-level expression of PD-1, PD-L1, NY-ESO-1, and MAGE-A4 could not be validated. Third, data interpretation was restricted to correlation analyses. Fourth, downstream signaling pathways and additional immune-related molecules were not examined. Finally, it remains unclear whether PD-L1, NY-ESO-1, and MAGE-A4 directly contribute to the pathogenesis of DT. Nevertheless, despite these constraints, the present study provides evidence supporting the involvement of PD-L1, NY-ESO-1, and MAGE-A4 in DT pathogenesis.

Conclusion

The NY-ESO-1/MAGE-A4 immune mechanism appears to exert a stronger influence than the PD-1/PD-L1 immune checkpoint pathway in the pathology of desmoid tumors, suggesting potential interaction between these mechanisms.

Conflicts of Interest

The Authors have no competing interests to declare in relation to this study.

Authors' Contributions

Conceptualization, K.H., S.N., H.T., and K.G.; methodology, K.H., S.N., and T.I.; software, K.H., T.I., and K.G.; validation, S.N., T.I., H.T., K.G., and K.H.; formal analysis, K.H., S.N., and T.I.; investigation, K.H., S.N., T.I., and K.G.; data curation, K.H., S.N., H.T., and K.G.; writing – original draft preparation, K.H., S.N., T.I., H.T., and K.G.; writing – review and editing, K.H., S.N., T.I., H.T., and K.G. All Authors have read and agreed to the published version of the manuscript.

Acknowledgements

The Authors acknowledge Chikoto Tanaka for providing technical assistance with the immunohistochemical staining procedures.

Funding

This study did not receive any dedicated funding from governmental, commercial, or non-profit organizations.

Artificial Intelligence (AI) Disclosure

No artificial intelligence (AI) tools, including large language models or machine learning software, were

used in the preparation, analysis, or presentation of this manuscript.

References

1 Ou J, Su D, Guan Y, Ge L, Deng S, Yan Y, Hao Y, Lu M, Zhang S, Xie R: Efficacy and safety of systemic treatment for progressive and refractory desmoid tumor: a systematic review and Bayesian network meta-analysis. Discov Oncol 15(1): 619, 2024. DOI: 10.1007/s12672-024-01494-z

2 McLean TD, Duchi S, Di Bella C: Molecular pathogenesis of sporadic desmoid tumours and its implications for novel therapies: a systematised narrative review. Target Oncol 17(3): 223-252, 2022. DOI: 10.1007/s11523-022-00876-z

3 Anderson WJ, Doyle LA: Updates from the 2020 World Health Organization Classification of Soft Tissue and Bone Tumours. Histopathology 78(5): 644-657, 2021. DOI: 10.1111/his.14265

4 Ascari F, Segattini S, Varoli M, Beghi M, Muratori S, Scotto B, Gasperoni M: Abdominal wall reconstruction for desmoid tumour surgery: Case report. Int J Surg Case Rep 64: 6-9, 2019. DOI: 10.1016/j.ijscr.2019.09.010

5 Siozopoulou V, Marcq E, Jacobs J, Zwaenepoel K, Hermans C, Brauns J, Pauwels S, Huysentruyt C, Lammens M, Somville J, Smits E, Pauwels P: Desmoid tumors display a strong immune infiltration at the tumor margins and no PD-L1-driven immune suppression. Cancer Immunol Immunother 68(10): 1573-1583, 2019. DOI: 10.1007/s00262-019-02390-0

6 Howard JH, Pollock RE: Intra-abdominal and abdominal wall desmoid fibromatosis. Oncol Ther 4(1): 57-72, 2016. DOI: 10.1007/s40487-016-0017-z

7 Mullen JT, DeLaney TF, Rosenberg AE, Le L, Iafrate AJ, Kobayashi W, Szymonifka J, Yeap BY, Chen YL, Harmon DC, Choy E, Yoon SS, Raskin KA, Hornicek FJ, Nielsen GP: β-Catenin mutation status and outcomes in sporadic desmoid tumors. Oncologist 18(9): 1043-1049, 2013. DOI: 10.1634/theoncologist.2012-0449

8 Yang W, Ding PR: Update on familial adenomatous polyposis-associated desmoid tumors. Clin Colon Rectal Surg 36(6): 400-405, 2023. DOI: 10.1055/s-0043-1767709

9 Aelvoet AS, Struik D, Bastiaansen BAJ, Bemelman WA, Hompes R, Bossuyt PMM, Dekker E: Colectomy and desmoid tumours in familial adenomatous polyposis: a systematic review and meta-analysis. Fam Cancer 21(4): 429-439, 2022. DOI: 10.1007/s10689-022-00288-y

10 Tayeb Tayeb C, Parc Y, Andre T, Lopez-Trabada Ataz D: [Familial adenomatous polyposis, desmoid tumors and Gardner syndrome]. Bull Cancer 107(3): 352-358, 2020. DOI: 10.1016/j.bulcan.2019.10.011

11 Eastley N, McCulloch T, Esler C, Hennig I, Fairbairn J, Gronchi A, Ashford R: Extra-abdominal desmoid fibromatosis: a review of management, current guidance and unanswered questions. Eur J Surg Oncol 42(7): 1071-1083, 2016. DOI: 10.1016/j.ejso.2016.02.012

12 Desmoid Tumor Working Group: The management of desmoid tumours: a joint global consensus-based guideline approach for adult and paediatric patients. Eur J Cancer 127: 96-107, 2020. DOI: 10.1016/j.ejca.2019.11.013

13 Dong H, Strome SE, Salomao DR, Tamura H, Hirano F, Flies DB, Roche PC, Lu J, Zhu G, Tamada K, Lennon VA, Celis E, Chen L: Tumor-associated B7-H1 promotes T-cell apoptosis: A potential mechanism of immune evasion. Nat Med 8(8): 793-800, 2002. DOI: 10.1038/nm730

14 Ghebeh H, Barhoush E, Tulbah A, Elkum N, Al-Tweigeri T, Dermime S: FOXP3+ Tregs and B7-H1+/PD-1+ T lymphocytes co-infiltrate the tumor tissues of high-risk breast cancer patients: Implication for immunotherapy. BMC Cancer 8: 57, 2008. DOI: 10.1186/1471-2407-8-57

15 Heppt MV, Heinzerling L, Kähler KC, Forschner A, Kirchberger MC, Loquai C, Meissner M, Meier F, Terheyden P, Schell B, Herbst R, Göppner D, Kiecker F, Rafei-Shamsabadi D, Haferkamp S, Huber MA, Utikal J, Ziemer M, Bumeder I, Pfeiffer C, Schäd SG, Schmid-Tannwald C, Tietze JK, Eigentler TK, Berking C: Prognostic factors and outcomes in metastatic uveal melanoma treated with programmed cell death-1 or combined PD-1/cytotoxic T-lymphocyte antigen-4 inhibition. Eur J Cancer 82: 56-65, 2017. DOI: 10.1016/j.ejca.2017.05.038

16 Akinleye A, Rasool Z: Immune checkpoint inhibitors of PD-L1 as cancer therapeutics. J Hematol Oncol 12(1): 92, 2019. DOI: 10.1186/s13045-019-0779-5

17 Salmaninejad A, Zamani MR, Pourvahedi M, Golchehre Z, Hosseini Bereshneh A, Rezaei N: Cancer/testis antigens: Expression, regulation, tumor invasion, and use in immunotherapy of cancers. Immunol Invest 45(7): 619-640, 2016. DOI: 10.1080/08820139.2016.1197241

18 Wang Y, Song X, Zheng Y, Liu Z, Li Y, Qian X, Pang X, Zhang Y, Yin Y: Cancer/testis antigen MAGEA3 interacts with STAT1 and remodels the tumor microenvironment. Int J Med Sci 15(14): 1702-1712, 2018. DOI: 10.7150/ijms.27643

19 Ravichandran R, Kodali K, Peng J, Potts PR: Regulation of MAGE-A3/6 by the CRL4-DCAF12 ubiquitin ligase and nutrient availability. EMBO Rep 20(7): e47352, 2019. DOI: 10.15252/embr.201847352

20 Alsalloum A, Shevchenko JA, Sennikov S: NY-ESO-1 antigen: A promising frontier in cancer immunotherapy. Clin Transl Med 14(9): e70020, 2024. DOI: 10.1002/ctm2.70020

21 Meng X, Sun X, Liu Z, He Y: A novel era of cancer/testis antigen in cancer immunotherapy. Int Immunopharmacol 98: 107889, 2021. DOI: 10.1016/j.intimp.2021.107889

22 Weon JL, Potts PR: The MAGE protein family and cancer. Curr Opin Cell Biol 37: 1-8, 2015. DOI: 10.1016/j.ceb.2015.08.002

23 Saito T, Wada H, Yamasaki M, Miyata H, Nishikawa H, Sato E, Kageyama S, Shiku H, Mori M, Doki Y: High expression of MAGE-A4 and MHC class I antigens in tumor cells and induction of MAGE-A4 immune responses are prognostic

markers of CHP-MAGE-A4 cancer vaccine. Vaccine 32(45): 5901-5907, 2014. DOI: 10.1016/j.vaccine.2014.09.002
24 Li S, Shi X, Li J, Zhou X: Pathogenicity of the MAGE family. Oncol Lett 22(6): 844, 2021. DOI: 10.3892/ol.2021.13105
25 Hashimoto K, Nishimura S, Ito T, Akagi M: Characterization of PD-1/PD-L1 immune checkpoint expression in soft tissue sarcomas. Eur J Histochem 65(3): 3203, 2021. DOI: 10.4081/ejh.2021.3203
26 Colombo C, Belfiore A, Paielli N, De Cecco L, Canevari S, Laurini E, Fermeglia M, Pricl S, Verderio P, Bottelli S, Fiore M, Stacchiotti S, Palassini E, Gronchi A, Pilotti S, Perrone F: β-Catenin in desmoid-type fibromatosis: deep insights into the role of T41A and S45F mutations on protein structure and gene expression. Mol Oncol 11(11): 1495-1507, 2017. DOI: 10.1002/1878-0261.12101
27 Kelany M, Barth TF, Salem D, Shakweer MM: Prevalence and prognostic implications of PD-L1 expression in soft tissue sarcomas. Pathol Oncol Res 27: 1609804, 2021. DOI: 10.3389/pore.2021.1609804
28 Kakimoto T, Matsumine A, Kageyama S, Asanuma K, Matsubara T, Nakamura T, Iino T, Ikeda H, Shiku H, Sudo A: Immunohistochemical expression and clinicopathological assessment of the cancer testis antigens NY-ESO-1 and MAGE-A4 in high-grade soft-tissue sarcoma. Oncol Lett 17(4): 3937-3943, 2019. DOI: 10.3892/ol.2019.10044
29 Hashimoto K, Nishimura S, Shinyashiki Y, Ito T, Tanaka H, Ohtani K, Kakinoki R, Akagi M: PD-1, PD-L1, NY-ESO-1, and MAGE-A4 expression in cutaneous angiosarcoma: A case report. Medicine (Baltimore) 101(28): e29621, 2022. DOI: 10.1097/MD.0000000000029621
30 Hashimoto K, Nishimura S, Ito T, Kakinoki R, Akagi M: Immunohistochemical expression and clinicopathological assessment of PD-1, PD-L1, NY-ESO-1, and MAGE-A4 expression in highly aggressive soft tissue sarcomas. Eur J Histochem 66(2): 3393, 2022. DOI: 10.4081/ejh.2022.3393